

Published in final edited form as:

*Opt Lett.* 2011 April 1; 36(7): 1299–1301.

## Compensation-free, all-fiber-optic, two-photon endomicroscopy at 1.55 $\mu\text{m}$

Kartikeya Murari<sup>1,†</sup>, Yuying Zhang<sup>1,†</sup>, Shenping Li<sup>2</sup>, Yongping Chen<sup>1</sup>, Ming-Jun Li<sup>2</sup>, and Xingde Li<sup>1,\*</sup>

<sup>1</sup>Department of Biomedical Engineering, Johns Hopkins University, 720 Rutland Avenue, Baltimore, Maryland 21205, USA

<sup>2</sup>Science and Technology, Corning Incorporated, Corning, New York 14831, USA

### Abstract

We present an all-fiber-optic scanning multiphoton endomicroscope with 1.55  $\mu\text{m}$  excitation without the need for prechirping femtosecond pulses before the endomicroscope. The system consists of a 1.55  $\mu\text{m}$  femtosecond fiber laser, a customized double-clad fiber for light delivery and fluorescence collection, and a piezoelectric scan head. We demonstrate two-photon imaging of cultured cells and mouse tissue, both labeled with indocyanine green. Free-space multiphoton imaging with near-IR emission has previously shown benefits in reduced background fluorescence and lower attenuation for the fluorescence emission. For fiber-optic multiphoton imaging there is the additional advantage of using the soliton effect at the telecommunication wavelengths (1.3–1.6  $\mu\text{m}$ ) in fibers, permitting dispersion-compensation-free, small-footprint systems. We expect these advantages will help transition multiphoton endomicroscopy to the clinic.

---

Multiphoton microscopy (MPM) is a widely used imaging technique in biology, particularly for its capability of optical sectioning without excessive photobleaching [1]. A recent development in the field has been the creation of fiber-optic endomicroscopes [2,3]. Such systems generally use a single optical fiber for light delivery and collection. The small footprint and flexibility of these devices have the potential for clinical translation of MPM, as well as new applications in basic scientific research.

Most multiphoton imaging, both free-space and fiber-optic, uses a femtosecond pulsed laser in the near-IR (NIR) region (typically 700 to 900 nm) to excite fluorophore, leading to emission in the visible region [4]. Free-space multiphoton microscopes have been demonstrated using Cr:Forsterite lasers around 1.23  $\mu\text{m}$  [5], Nd:YLF pumped optical parametric oscillator (OPO) sources around 1.45–1.63  $\mu\text{m}$  [6], Ti:Sapphire pumped OPOs at 1.06–1.45  $\mu\text{m}$  [7], and Erbium-doped fiber lasers at 1.55  $\mu\text{m}$  [8]. Advantages of longer wavelength excitation include deeper penetration of the excitation light, due to reduced tissue scattering, and emission in the NIR window with reduced tissue absorption and scattering and considerably reduced background autofluorescence. However, these advantages come with the caveats of higher water absorption at the excitation wavelength and lower resolution due to the increase in the diffraction-limited focused spot size (for a given NA of the imaging objective lens).

Another major advantage of longer wavelength excitation, particularly for fiber-optic multiphoton endomicroscopy, is the ease of dispersion management of femtosecond pulses in the region of 1.3–1.6  $\mu\text{m}$ . It is relatively straightforward to make optical fibers with anomalous dispersion in this wavelength region, making it possible to utilize the soliton effect to minimize the distortion of the ultrashort pulses in a fiber-optic endomicroscope, which eliminates the requirement of pulse prechirping before launching the pulses into the endomicroscope. Since dispersion management is not required, the size and complexity of MPM endomicroscopes can be dramatically reduced, and a turnkey operation may be possible using a compact femtosecond fiber laser. In addition, the cost of MPM endomicroscopes can be significantly reduced due to the wide availability of generic, low-cost fiber-optic telecommunication components in the wavelength range of 1.3–1.6  $\mu\text{m}$ . In this Letter, we present a compensation-free, all-fiber-optic scanning endomicroscope using a single double-cladding fiber for 1.55  $\mu\text{m}$  pulsed laser delivery and two-photon excited fluorescence collection. To the best of our knowledge this is the first report of an all-fiber-optic MPM system with NIR fluorescence emission.

The reported two-photon fluorescence endomicroscopy system utilizes a 1.55  $\mu\text{m}$  femtosecond fiber laser. Figure 1(a) shows a block diagram of the laser, which consists of a seed laser, a fiber-based pulse stretcher, a customized Er-doped fiber amplifier (EDFA) (PolarOnyx Inc.), and a fiber-based pulse compressor. The seed laser was a 1.55  $\mu\text{m}$  passively mode-locked fiber laser that generated  $\sim 1$  ps, 42.5 MHz pulses with a 3 dB spectral bandwidth of  $\sim 30$  nm and an average power of  $\sim 2$  mW. The pulse stretcher was a 110-m-long, customized (Corning Inc.), dispersion-shifted single-mode fiber with normal dispersion at 1.55  $\mu\text{m}$ . The total dispersion of the stretcher was about  $-10$  ps/nm. The seed pulses were stretched to about 290 ps after the fiber stretcher and then amplified by the EDFA up to an average power of about 160 mW. Finally, the pulses were launched into the fiber compressor, which used both fiber chromatic dispersion and soliton effect [9,10] to compress the pulses. The pulse compressor was a 700-m-long SMF-28 fiber with anomalous dispersion at 1.55  $\mu\text{m}$ , totaling about 12.3 ps/nm. To form a soliton (and thus preserve the pulse shape over a certain distance), the dispersion of the stretcher (e.g., with a negative dispersion parameter  $D$ ) was smaller than that of the compressor (with a positive dispersion parameter  $D$ ). The output pulses from the fiber stretcher could be compressed to below 300 fs (assuming a  $\text{sech}^2$  pulse shape) with a power up to 155 mW. The laser emission was nonpolarized, and the numerical aperture of the output fiber was 0.13.

The details of the endomicroscope setup are shown in Fig. 1(b). The front end of the system consisted of a 2 mm diameter scanning probe with a four-quadrant tubular piezoelectric actuator [2]. A customized 70-cm-long double-clad fiber (DCF) (Corning Inc.) was passed through and glued to the actuator with an  $\sim 1$  cm free-standing length to serve as a fiber-optic cantilever for beam scanning. The outer diameter of the DCF was 180  $\mu\text{m}$ , with core and inner cladding diameters of 8 and 175  $\mu\text{m}$ , respectively [see Fig. 1(c)]. The core and inner cladding NAs of the fiber were 0.12 and 0.267, respectively. The core carried excitation light, while the fluorescence was collected by the inner cladding (plus the core). At the end of the probe, a miniature compound lens made of two aspheric lenses (LightPath Cat. 370840 and 370940) was used for focusing the excitation light with an NA of 0.8 (on the sample side) and a working distance of  $\sim 200$   $\mu\text{m}$  in air, with a configuration similar to what we reported previously [11]. Ray-tracing simulations indicated a chromatic focal shift of 670  $\mu\text{m}$  between the 1.55  $\mu\text{m}$  excitation and 800 nm emission. Following the direction of the excitation light, the free-space optical setup before the endomicroscope consisted of a collimator, two silver mirrors, a customized dichroic mirror with reflectivity  $>99.97\%$  from 0.7–0.9  $\mu\text{m}$  to separate the fluorescence emission from the excitation, an aspheric coupling lens ( $f = 6$  mm, NA 0.4), and a photomultiplier tube (PMT) sensitive from 300 to 900 nm

(Hamamatsu R7400) with a collection lens and a 700 nm long-pass filter (Edmund Optics) to reject ambient light.

Figure 2 shows characterization data for the laser alone, as well as for the entire endomicroscopy system. Figure 2(a) shows the spectra at the output of the laser and at the output of the endomicroscope after delivery through the free-space optics and the DCF. Figure 2(b) shows autocorrelation traces measured at the same two locations. Since the dispersion and the mode field diameter of the DCF and the compressor fiber (SMF-28) are similar, the DCF can be considered as a part of the compressor. The pulse shape thus remains relatively unchanged through the DCF due to the short length of the DCF. Assuming a  $\text{sech}^2$  pulse shape, the measurements indicated about 5% pulse broadening.

Two-photon fluorescence imaging studies were performed to test the performance of the scanning endomicroscope equipped with the short-pulsed 1.55  $\mu\text{m}$  fiber laser. The scanning range of the fiber tip was  $\sim 490 \mu\text{m}$ , resulting in a 110  $\mu\text{m}$  field of view on samples.

The fluorescent dye used for imaging was indocyanine green (ICG), which has a single-photon excitation peak at 780 nm and an emission peak at 830 nm. An average power between 30 and 50 mW on the samples was used for imaging. Two forms of the dye were used—a 10  $\mu\text{M}$  aqueous solution of ICG and antibody conjugated ICG micelles.

The *in vitro* imaging study involved A431 cells cultured on coverslips in six-well plates at a density of  $2 \times 10^5$  cells/well in Dulbecco's modified Eagle's medium with 10% fetal bovine serum and 1% penicillin:streptomycin. Cells achieved an 80% confluency after 3 days. ICG micelles were synthesized as described elsewhere [12,13] and conjugated with anti-epidermal growth factor receptor (anti-EGFR) antibodies [14]. EGFR is a membrane protein that is overexpressed on the A431 cell membrane. Prior to imaging, cells were incubated with anti-EGFR conjugated ICG micelles for 3 h. Samples were washed thrice in phosphate buffered saline before imaging. Figures 3(a) and 3(b) show representative two-photon fluorescence images of the cells acquired with the scanning endomicroscope at an imaging speed of  $\sim 2.6$  frames per second. The cell membranes, lit up by the bioconjugated ICG micelles, were evident.

For tissue imaging, 50  $\mu\text{L}$  of 10  $\mu\text{M}$  aqueous ICG solution was injected into the tail vein of an 8-week-old nude mouse. The mouse was also given an intramuscular (i.m.) injection of 50  $\mu\text{L}$  ICG solution (10  $\mu\text{M}$ ) to locally stain tissue. In the blood, ICG rapidly binds to plasma proteins and does not extravasate. It has a half-life of 150–180 s and is cleared from the circulation exclusively by the liver via the biliary pathway [15]. The mouse was sacrificed 15 min after ICG administration, and the bile duct and the muscle around the i.m. injection site were resected and then imaged with the endomicroscope. Figure 3(c) shows a representative image of the bile duct indicating accumulation of ICG in the duct. Figure 3(d) shows a representative two-photon fluorescence image, in which a muscle fiber can be clearly visualized with characteristic transverse striations caused by sarcomeres. Z-scan imaging indicated that an  $\sim 150 \mu\text{m}$  imaging depth could be achieved.

In summary, we have demonstrated an all-fiber-optic scanning multiphoton endomicroscope integrated with a femtosecond fiber laser at 1.55  $\mu\text{m}$  that was capable of imaging NIR fluorescent probes like ICG. Benefits of operation in this wavelength range include minimal autofluorescence and potentially better imaging depth due to both the excitation and emission being in the NIR window with reduced overall tissue attenuation. For fiber-optic systems, there is the additional advantage of the synergistic effects of self-phase modulation and anomalous dispersion, leading to minimal pulse distortion. This allows for operation without prechirping the pulses, thus greatly reducing the complexity and footprint of the

entire imaging system. Such systems, combined with a compact turnkey femtosecond fiber laser and well-developed optical components at NIR telecommunication wavelengths, have the potential to transform the current powerful but expensive MPM systems to a low-cost endomicroscopy platform for not only basic science laboratories but also the clinic. Future studies might focus on the thermal effect associated with the increased water absorption at 1.55  $\mu\text{m}$ .

## Acknowledgments

The authors would like to thank Jiefeng Xi in our group, Jian Liu and Lih-Mei Yang at PolarOnyx Inc., and Michael Holmes at Toptica Inc. for their technical assistance in this work. This research was supported in part by the National Institutes of Health (NIH) (R01 CA120480, R01 CA153023, and R01 EB007636) and the National Science Foundation (NSF) (Career Award—XDL).

## References

1. Denk W, Strickler JH, Webb WW. *Science*. 1990; 248:73. [PubMed: 2321027]
2. Myaing MT, MacDonald DJ, Li XD. *Opt Lett*. 2006; 31:1076. [PubMed: 16625908]
3. Fu L, Jain A, Xie H, Cranfield C, Gu M. *Opt Express*. 2006; 14:1027. [PubMed: 19503423]
4. Xu C, Webb WW. *J Opt Soc Am B*. 1996; 13:481.
5. Chu SW, Chen IH, Liu TM, Chen PC, Sun CK, Lin BL. *Opt Lett*. 2001; 26:1909. [PubMed: 18059734]
6. McConnell G. *Phys Med Biol*. 2007; 52:717. [PubMed: 17228116]
7. Andresen V, Alexander S, Heupel WM, Hirschberg M, Hoffman RM, Friedl P. *Curr Opin Biotechnol*. 2009; 20:54. [PubMed: 19324541]
8. Yazdanfar S, Joo C, Zhan C, Berezin MY, Akers WJ, Achilefu S. *J Biomed Opt*. 2010; 15:030505. [PubMed: 20614991]
9. Chan KC, Liu HF. *IEEE J Quantum Electron*. 1995; 31:2226.
10. Gouveia-Neto A, Gomes A, Taylor J. *IEEE J Quantum Electron*. 1987; 23:1193.
11. Wu YC, Xi JF, Cobb MJ, Li XD. *Opt Lett*. 2009; 34:953. [PubMed: 19340182]
12. Rodriguez VB, Henry SM, Hoffman AS, Stayton PS, Li XD, Pun SH. *J Biomed Opt*. 2008; 13:014025. [PubMed: 18315383]
13. Kim TH, Chen YP, Mount CW, Gombotz WR, Li XD, Pun SH. *Pharm Res*. 2010; 27:1900. [PubMed: 20568000]
14. Chen, Y.; Jabbour, TG.; Li, X. OSA Technical Digest (CD). Optical Society of America; 2010. Biomedical Optics. paper BTuC6
15. Cherrick GR, Stein SW, Leevy CM, Davidson CS. *J Clin Invest*. 1960; 39:592. [PubMed: 13809697]

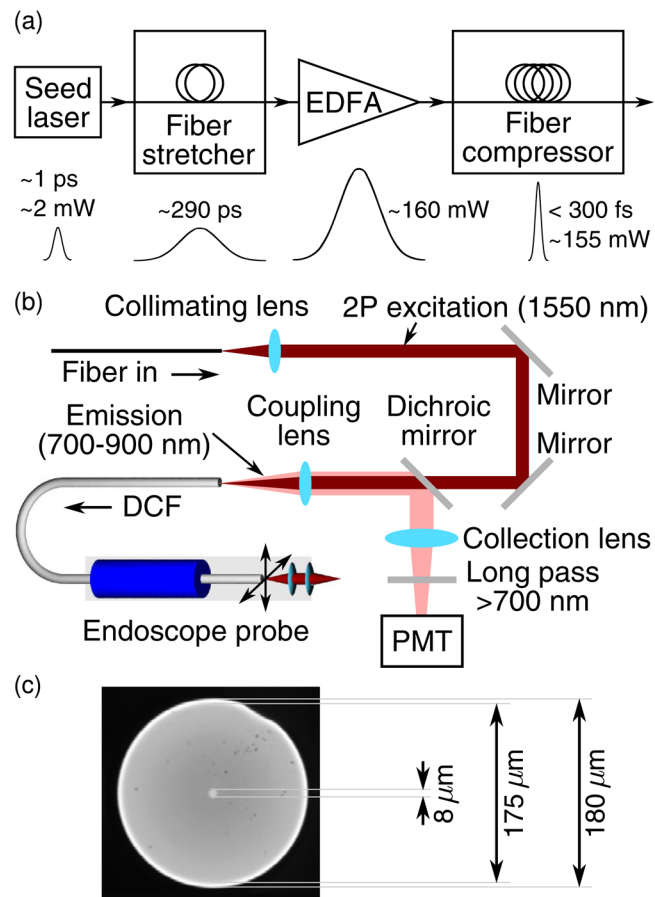


**Fig. 1.** (Color online) System design and components: (a) block diagram of the 1.55  $\mu\text{m}$  short-pulsed fiber laser, (b) detailed layout of the optical path, (c) micrograph of the double-clad fiber cross section.

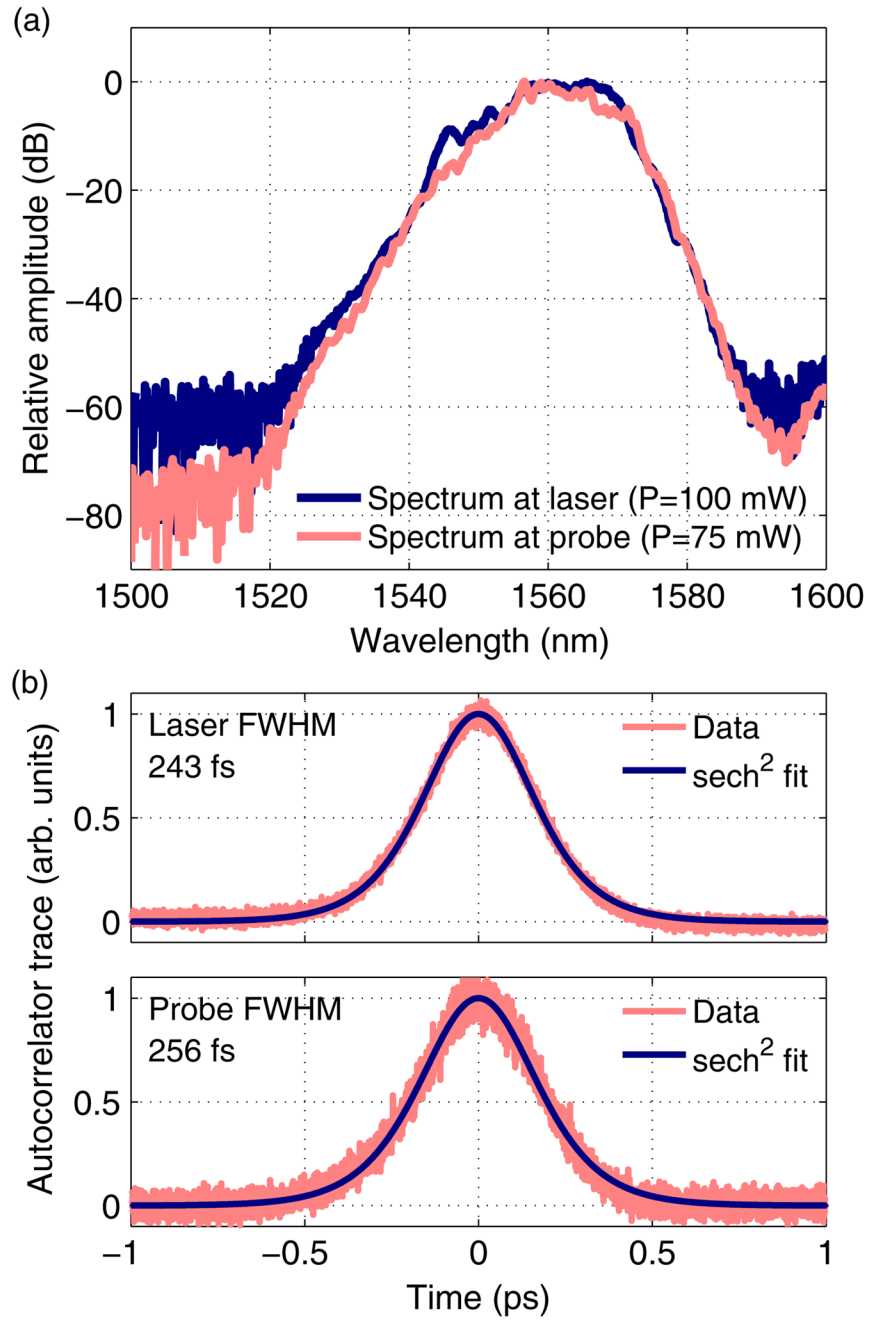


**Fig. 2.** (Color online) (a) Spectra and (b) autocorrelation traces of the pulses at the laser output and at the endomicroscope output.

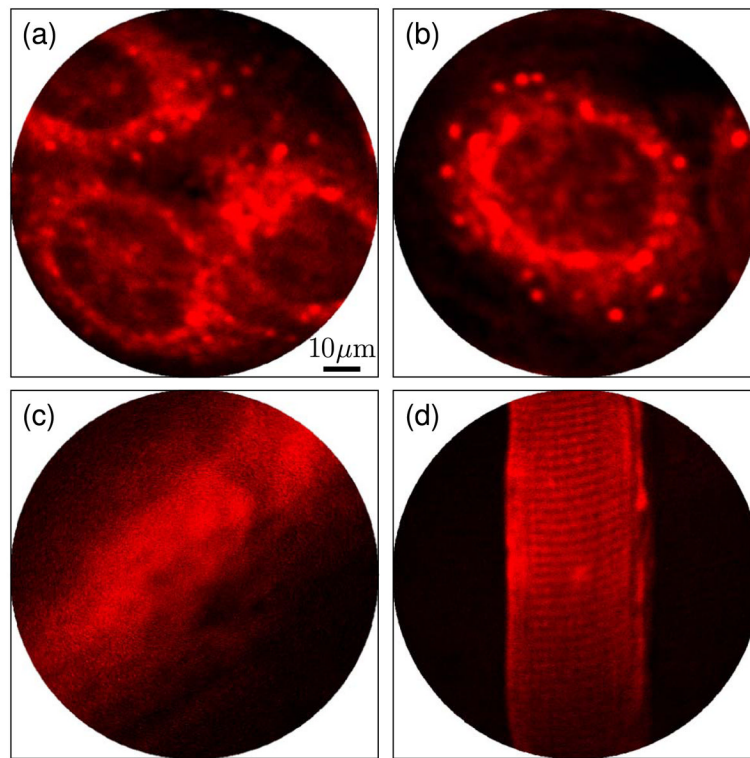


**Fig. 3.** (Color online) Multiphoton fluorescence images (averaged five times) with  $1.55 \mu\text{m}$  excitation. (a), (b) A431 cells targeted with anti-EGFR antibody conjugated ICG micelles, (c) *ex vivo* mouse bile duct after tail vein administration of  $50 \mu\text{L}$  ICG solution ( $10 \mu\text{M}$ ), (d) skeletal muscle after i.m. administration of  $50 \mu\text{L}$  ICG solution ( $10 \mu\text{M}$ ) showing characteristic striations.